PHYSICAL REVIEW A **85**, 040305(R) (2012)

Cascaded entanglement enhancement

Zhihui Yan (闫智辉), Xiaojun Jia (贾晓军),* Xiaolong Su (苏晓龙), Zhiyuan Duan (段志园), Changde Xie (谢常德), and Kunchi Peng (彭堃墀)

State Key Laboratory of Quantum Optics and Quantum Optics Devices, Institute of Opto-Electronics, Shanxi University, Taiyuan, 030006, People's Republic of China

(Received 4 January 2012; published 16 April 2012)

We present a cascaded system consisting of three nondegenerate optical parametric amplifiers (NOPAs) for the generation and the enhancement of quantum entanglement of continuous variables. The entanglement of optical fields produced by the first NOPA is successively enhanced by the second and the third NOPAs from −5.3 to −8.1 dB below the quantum noise limit. The dependence of the enhanced entanglement on the physical parameters of the NOPAs and the reachable entanglement limitation for a given cascaded NOPA system are calculated. The calculation results are in good agreement with the experimental measurements.

DOI: 10.1103/PhysRevA.85.040305 PACS number(s): 03.67.Bg, 42.50.Dv, 03.65.Ud, 42.50.Lc

Nonlocal quantum entanglement is the key resource to realize quantum information processing (QIP) [1–3]. The entangled states of single photons (qubits) and optical modes (qumodes) have been applied in QIP with discrete and continuous variable (DV and CV) regimes, respectively [4,5]. The Einstein-Podolsky-Rosen (EPR) [6] entangled states of an optical field are the essential quantum resources for implementing CV QIP. In the quantum optics the quadrature amplitude and the quadrature phase play the roles of the canonical position and momentum variables in the original EPR proposal [7]. The optical EPR state is a two-mode entangled state consisting of two submodes with quantum correlations between both quadrature amplitude and quadrature phase. If the experimentally measured combination of the fluctuation variances for the amplitude sum (difference) and the phase difference (sum) of the two submodes is smaller than the corresponding quantum noise limit (QNL), the two optical submodes are inseparable and thus form an optical state with EPR entanglement [7–9]. The quadrature squeezed states of light are the necessary basis to establish quantum entanglement among optical fields [10]. A scheme of generating CV optical entangled states is to interfere two single-mode squeezed states of light with an identical frequency and a constant phase difference on a 50 : 50 beam splitter [5,11]. The two single-mode squeezed states are often produced by a pair of degenerate optical parametric amplifiers (DOPAs) with an identical type-I nonlinear crystal pumped by a laser to ensure high interference efficiency. Through careful technical improvements in suppressing the phase fluctuation of optical field and by reducing the intracavity losses of the DOPA, the squeezing level of the single-mode squeezed states has been continually renewed in recent years [12–16]. So far, a squeezing over −12 dB below QNL has been achieved by a group in Hannover [13,15]. Coupling a single-mode squeezed state of −9.9 dB and a vacuum field on a 50 : 50 beam splitter, the EPR entangled state of light with a quantum correlation of amplitude and phase quadratures of −3 dB below the QNL was obtained in 2011 [16]. The four-mode CV entanglement of −6 dB below the QNL was achieved by combining four initial single-mode squeezed states generated by four DOPAs [17].

Another important device to generate a CV EPR entangled state of an optical field is the nondegenerate optical parametric amplifier (NOPA) consisting of an optical cavity and a type-II nonlinear crystal. Through the intracavity frequency-downconversion process in a NOPA, a pair of nondegenerate optical modes with amplitude and phase quadrature correlations is directly produced, which is an EPR entangled state [18–20]. Twenty years ago, Kimble's group experimentally generated a pair of CV entangled optical beams with a NOPA and demonstrated the EPR paradox first in the CV regime [18]. Then, NOPAs operating at a different version (above or lower than the threshold, amplification or deamplification) are used as sources for generating optical CV entangled states and the produced EPR beams are applied in a variety of CV QIP experiments [19–24]. However, for a long time the EPR entanglement level was kept around −4 dB or lower [18–24]. Until 2010, after a series of strictly technical improvements on the NOPA system, the EPR entanglement degree was raised to −6 dB [25], which, to the best our knowledge, was the best reported result on the NOPA system. In principle, according to the generally theoretical model, without considering the influences of extra phase noise on the antisqueezing quadrature, the entanglement of the output field from a NOPA is limited fundamentally only by its escape efficiency (the ratio of the transmissivity efficiency to the sum of the transmissivity efficiency and the intracavity loss) and the pump parameter (the ratio of the pump power to the pump threshold). For a given NOPA with a certain escape efficiency, we could raise the entanglement by increasing the pump power. However, in a practical system there always is unavoidable extra phase noise and the thermal effects of the nonlinear crystal, which increase along with the pump power. To keep the NOPA stable and degrade the influence of extra noise, usually the pump parameters are limited between 60% and 75%, which are the optimal pump parameters of each NOPA for producing a stable and possibly highest entanglement [12–16,19,20,25].

To further raise entanglement under generally technical conditions, we design the cascaded NOPA system involving three NOPAs and experimentally realized the cascaded amplification of CV entanglement. The initial EPR entanglement of

*jiaxj@sxu.edu.cn

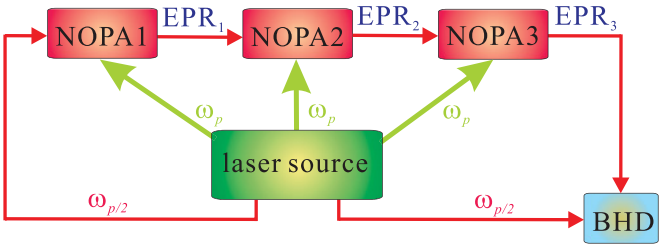

FIG. 1. (Color online) The principle schematic of the cascaded entanglement enhancement system.

−5.3 dB produced by the first NOPA (NOPA1) is enhanced to −7.2 dB by the second one (NOPA2) and successively to −8.1 dB by the third one (NOPA3), which is the highest EPR entanglement of optical modes obtained by experiments so far, to the best of our knowledge. We numerically calculate the correlation variances of the enhanced EPR entangled state based on the physical parameters of the experimental system. The calculated results are in good agreement with the experimental measurements.

Figure 1 shows the principle schematic of the cascaded entanglement enhancement system. The laser source is an intracavity frequency-doubled cw laser, from which the output second-harmonic wave (ω_p) is used for the pump fields of the three NOPAs and the output fundamental wave ($\omega_{p/2}$) serves as the injected signal of NOPA1, and the local oscillator (LO) of the balanced homodyne detector (BHD) for the entanglement measurement. The EPR entangled light generated by NOPA1 (EPR1) is injected into NOPA2 as the injected signal for the first-stage enhancement of the entanglement and the amplified EPR optical field (EPR2) is injected into NOPA3 for the second-stage enhancement. The final entangled light (EPR3) is detected by the BHD. Only when the three NOPAs are operated simultaneously in a deamplification situation or in an amplification situation can cascaded entanglement enhancement be achieved. Otherwise, the entanglement of the injected seed field will be degraded by the next NOPA operating in the opposite situation [26,27]. In the presented experiment, the three NOPAs are operated below the oscillation threshold of NOPA and in the deamplification situation, i.e., the pump field and the injected signal are out of phase [with the phase difference of $(2n+1)\pi$, n integer]. In this case the entangled states produced have a correlated amplitude sum and phase difference as well as an anticorrelated amplitude difference and phase sum [19–21].

In the following first we calculate the correlation variances between the amplitude and phase quadratures of the EPR entangled state enhanced by a NOPA. We describe the quantum state of light with the electromagnetic field annihilation operators $\hat{a} = (\hat{X} + i\hat{Y})/2$, where $\hat{X}$ and $\hat{Y}$ are the operators of the amplitude ($\hat{X}$) and the phase ($\hat{Y}$) quadratures, respectively. $\hat{X}$ and $\hat{Y}$ satisfy the canonical commutation relation $[\hat{X},\hat{Y}] = 2i$. The correlation variances and the anticorrelation variances of the injected EPR optical modes, which are produced by the former NOPA, are expressed by $\langle\delta^2(\hat{X}^{\rm in}_{a_1} + \hat{X}^{\rm in}_{a_2})\rangle = \langle\delta^2(\hat{Y}^{\rm in}_{a_1} - \hat{Y}^{\rm in}_{a_2})\rangle = 2e^{-2r}$ and $\langle\delta^2(\hat{X}^{\rm in}_{a_1} - \hat{X}^{\rm in}_{a_2})\rangle = \langle\delta^2(\hat{Y}^{\rm in}_{a_1} + \hat{Y}^{\rm in}_{a_2})\rangle = 2e^{2r+2r'}$, where r and r' are the correlation parameter and the extra noise factor on the anticorrelation components, respectively; $\hat{X}^{\rm in}_{a_{1(2)}}$ and $\hat{Y}^{\rm in}_{a_{1(2)}}$ stand for the amplitude and the phase quadratures of the injected mode $\hat{a}^{\rm in}_{1(2)}$, respectively [26,28]. Here, we have supposed that the signal and idler modes are balanced, which is easily satisfied in experiment [18–21]. Solving the quantum Langevin motion equations and using the input-output relation of the NOPA, the correlation variances of the output field are obtained:

$$\begin{aligned}
&\left\langle\delta^2\left(\hat{X}^{\rm out}_{a_1} + \hat{X}^{\rm out}_{a_2}\right)\right\rangle \\
&= \left\langle\delta^2\left(\hat{Y}^{\rm out}_{a_1} - \hat{Y}^{\rm out}_{a_2}\right)\right\rangle = \left\{\zeta\left[2\frac{(-\kappa+\gamma_1-\gamma_2)^2+(\omega\tau)^2}{(\kappa+\gamma_1+\gamma_2)^2+(\omega\tau)^2}e^{-2r}\right.\right. \\
&\quad \left.\left. + \frac{8\gamma_1\gamma_2}{(\kappa+\gamma_1+\gamma_2)^2+(\omega\tau)^2}\right] + 1 - \zeta\right\}\cos^2\theta \\
&\quad + \left\{\zeta\left[2\frac{(-\kappa+\gamma_1-\gamma_2)^2-(\omega\tau)^2}{(\kappa+\gamma_1+\gamma_2)^2+(\omega\tau)^2}e^{2r+2r'}\right.\right. \\
&\quad \left.\left. + \frac{8\gamma_1\gamma_2}{(\kappa+\gamma_1+\gamma_2)^2+(\omega\tau)^2}\right] + 1 - \zeta\right\}\sin^2\theta, \qquad (1)
\end{aligned}$$

where $\hat{X}^{\rm out}_{a_{1(2)}}$ and $\hat{Y}^{\rm out}_{a_{1(2)}}$ are the amplitude and the phase quadratures of the output mode $\hat{a}^{\rm out}_{1(2)}$, respectively; γ_1 and γ_1 are the transmissivity efficiency and the intracavity loss of the NOPA; $\kappa = \beta\chi$ is the nonlinear coupling efficiency of the NOPA, which is proportional to the pump parameter $\beta = (p_{\rm pump}/p_{\rm th})^{1/2}$ ($p_{\rm pump}$ is the pump power, and $p_{\rm th}$ is the threshold pump power of NOPA) and the second-order nonlinear coupling coefficient χ of the nonlinear crystal used in the NOPA; τ is the roundtrip time of light in the optical cavity; $\omega = 2\pi\Omega$ is the noise analysis frequency; ζ is the imperfect detection efficiency; and θ is the relative phase fluctuation between the pump field and the injected signal resulting from imperfect phase locking.

Figure 2(a) is the calculated dependence of correlation variances of the output EPR optical field from NOPA3 on the cavity parameter γ_1 and γ_2, where other parameters are taken according to the experimental system ($r = 0.83$, $r' = 0.45$, which correspond to the entanglement degree of EPR2 with a correlation variance of −7.2 dB below the QNL and the anticorrelation variance of 11.1 dB above the QNL; see the experimental results in the text; $\theta = 0.0105$; $\Omega = 2.0$ MHz; $\tau = 2.0\times10^{-9}$ s; $\varsigma = 0.947$). When γ_1 increases and γ_2 decreases, the correlation variance of the output field reduces, i.e., the entanglement degree increases. It means that, for a simple NOPA, the higher input-output transmissivity (γ_1) and the lower intracavity loss (γ_2) can provide a stronger performance of the entanglement enhancement. However, for a NOPA with given physical parameters, the correlation variances of the output field depend on the correlation variances of the injected signal field. Figure 2(b) shows the functions of the correlation variances of the output field versus those of the input field, where trace (i) for $\gamma_1 = 0.1$, $\gamma_2 = 0.004$ and trace (ii) for $\gamma_1 = 0.1$, $\gamma_2 = 0.001$; the other parameters are the same as those of Fig. 2(a). We can see from Fig. 2(b) that there is a turning point in trace (i) (−8.5 dB) and (ii) (−10.0 dB), respectively, where the correlation variance of the output field is equal to that of the input field. After the turning point the correlation variances of the output field

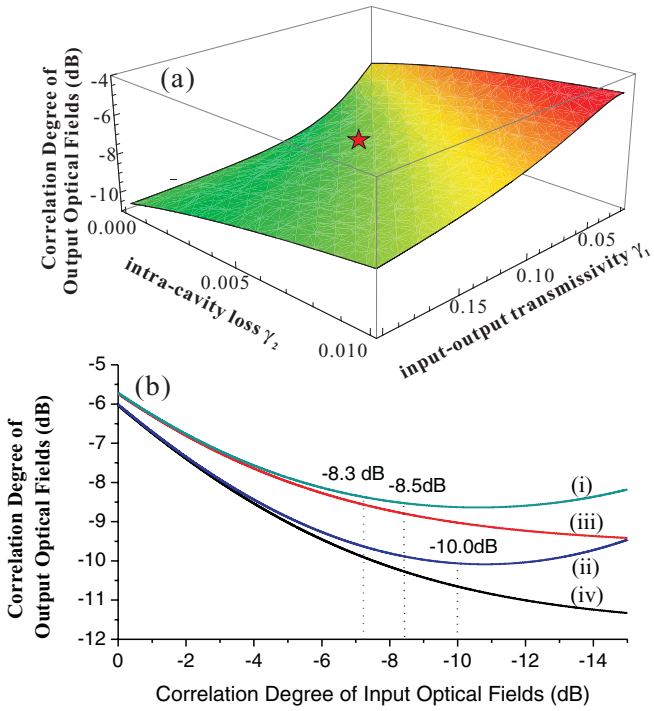

FIG. 2. (Color online) (a) The dependence of correlation variances of the output entangled optical field on the input-output transmissivity γ_1 and the intracavity loss γ_2 of NOPA. (b) The functions of the correlation variances of the output field vs those of the input field for two NOPAs: (i) $\gamma_1 = 0.1, \gamma_2 = 0.004, \theta = 0.0105$; (ii) $\gamma_1 = 0.1, \gamma_2 = 0.001, \theta = 0.0105$; (iii) $\gamma_1 = 0.1, \gamma_2 = 0.004, \theta = 0$; (iv) $\gamma_1 = 0.1, \gamma_2 = 0.001, \theta = 0$.

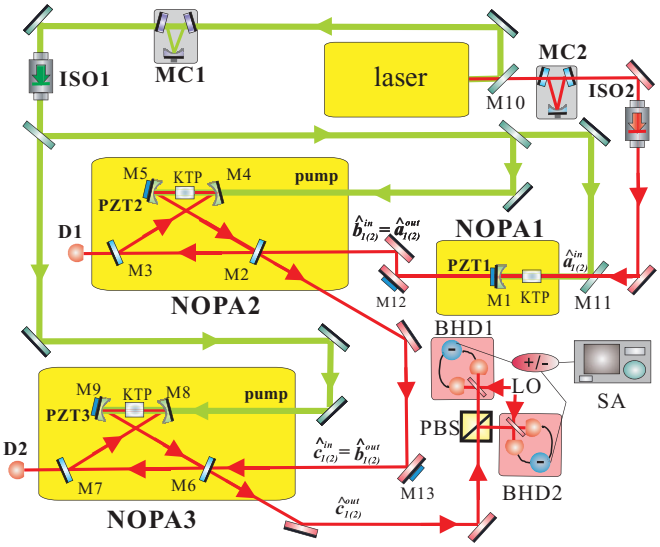

FIG. 3. (Color online) The experimental setup of cascade sensitive-phase entanglement enhancement: laser, Nd:YAP/LBO laser source; PBS, polarizing beam splitter; MC1(2), mode cleaner; ISO1(2), optical isolator; M0–M13, different mirrors (see text for details); PZT, piezoelectric transducer; D1(2), photodetector; +/−, positive/negative power combiner; SA, spectrum analyzer.

will be larger than those of the input signal. It means the enhancement ability of the NOPA no longer exists. Comparing traces (i) and (ii), it is obvious that the NOPA with the smaller intracavity loss [trace (ii)] has a stronger ability for entanglement enhancement. This is because the noise of the anticorrelation components in the input field increases rapidly along with an increase of the correlation degree, and the noise on the anticorrelation components would be inevitably coupled to the correlation component and thus decrease the correlation degree of the output fields due to the existence of the phase fluctuation θ in the experimental system [see the second term of Eq. (1)]. Reducing the phase fluctuation in the phase-locking system, the upper limitation of the input field for the entanglement enhancement will be raised. For the ideal case of $\theta = 0$ the turning point will vanish [see curves (iii) and (iv) of Fig. 2(b)].

The experimental setup is shown in Fig. 3. A continuous-wave intracavity frequency-doubled and frequency-stabilized Nd:YAP/LBO (Nd-dropped $YAlO_3/LiB_3O_5$) laser (Yuguang Co. Ltd., FG-VIB) with both a harmonic-wave output at 540 nm and the subharmonic-wave output at 1080 nm serving as the laser sources of the entanglement enhancement system. The output green and infrared lasers are separated by a beam splitter M10 coated with high reflection for 540 nm and high transmission for 1080 nm. The green laser serves as the pump field for three NOPAs and the infrared laser is used for the injected signal of NOPA, as well as the local oscillators (LO) of BHD1 and BHD2. The traveling-wave mode cleaners (MC1 for 540 nm and MC2 for 1080 nm) consisting of three mirrors are used for the optical low-pass filters of noises and the spatial mode cleaners. The finesses of MC1 for 540 nm and MC2 for 1080 nm are both 550. The optical isolators (ISO1 for 540 nm and ISO2 for 1080 nm) are utilized to prevent the feedback optical fields from the NOPA from returning to the laser. We choose the α-cut type-II KTP ($KTiOPO_4$) to be the nonlinear medium in the three NOPAs, which can achieve type-II noncritical phase-matched frequency downconversion of the pump field at 1080 nm. The size of the three KTP crystals is the same ($3 \times 3 \times 10$ mm^3) and temperature of the KTP crystal in the three NOPAs is controlled around 63 °C to satisfy the phase-matching condition. Since the phase-matching temperature of KTP has a broad full width of about 30 °C, we can make the signal and the idler modes double resonate inside a NOPA by carefully tuning the temperature of the crystal around 63 °C. The NOPA1 is in a semimonolithic Fabry-Pérot configuration consisting of a KTP crystal and a concave mirror (M1) with a 50-mm radius of curvature. The front face of the crystal is coated to be used as the input coupler of the pump field (the transmissivity of 99.8% at 540 nm and 0.04% at 1080 nm), and the other face is coated with dual-band antireflection at both 540 and 1080 nm. M1 coated with a transmissivity of 5.2% at 1080 nm and high reflection at 540 nm is used as the output coupler and is mounted on a piezoelectric transducer (PZT1) to scan actively the cavity length of NOPA1 or lock it on resonance with the injected signal as needed. However, due to the existence of the unavoidable extra phase noises, the relative phase between the pump field and the injected seed light is not able to be locked exactly at the required value (0 or π) and there always is a phase fluctuation θ around the

locked value. The value of θ can be experimentally detected by measuring the rms noise of the error signals on locked operation [29]. The length and the finesse of the cavity of NOPA1 are 54 mm and 115, respectively. The NOPA2 (3) has a ring configuration consisting of two flat mirrors M2 (6) and M3 (7) and two concave mirrors M4 (8) and M5 (9) with a 100-mm radius of curvature. The KTP crystal with 1080- and 540-nm dual-band antireflection coated at both end faces is placed in the middle of M4 (8) and M5 (9). M2 (6) serves as the input-output coupler with a transmission of 10.0% at 1080 nm and antireflection at 540 nm, respectively. All the other mirrors are high reflection at 1080 nm and antireflection at 540 nm. M5 (9) is mounted on PZT2 (3) for scanning or locking actively the length of the optical cavity NOPA2 (3). The length and the finesse of the cavity for both NOPA2 and NOPA3 are 557 mm and 60, respectively. The threshold pump powers of the three NOPAs are 250 mW for NOPA1 and 900 mW for NOPA2 and NOPA3, respectively. To lock the relative phase between the injected seed and the pump light of NOPA2 (3) to the deamplification point, we phase modulate the seed light using a dither signal of 37 kHz (41 kHz) by means of the PZT mounted on M12 (13). Then we monitor the intensity of the leaked seed light from the cavity mirror M3 (7) with the photodetector D1 (D2) and make the intensity minimum, i.e., the relative phase equals π by controlling the PZT on M12 (13). In this case, we demodulate the modulated dither signal on the output of D1 (2) and feedback the error signal to the PZT on M12 (13) to lock the parametric gain of NOPA2 (3) at the deamplification point. However, there is always the phase fluctuation in real experiments which will unavoidably influence the phase-locking precision. The measured fluctuation of θ around π is about 0.0105 for our experimental system. From the second term of Eq. (1) we can see that the influence of the θ fluctuation on the entanglement enhancement depends on the entanglement degree of the injected seed light. The higher the initial entanglement is, the stronger is the influence. The signal and the idler optical beams with orthogonal polarizations produced by NOPA3 are separated by a polarizing beam splitter (PBS) and then are detected by BHD1 and BHD2, respectively. The BHD consists of a 50 : 50 beam splitter and a pair of photodiodes (ETX-500 InGaAs). Locking the relative phase between the signal (idler) beam and the LO to 0 or $\pi/2$, the fluctuations of amplitude or phase quadrature of the signal (idler) field can be measured by BHD1 (2). The noise powers of the amplitude (phase) quadratures simultaneously measured by BHD1 and BHD2 are combined by the positive (negative) power combiner [$\oplus(\ominus)$] and then the correlation variances of the amplitude sum (phase difference) are analyzed by a spectrum analyzer (SA).

Figures 4(a) and 4(b) show the measured correlation variances of the amplitude sum and the phase difference, respectively. In Fig. 4(a) [Fig. 4(b)] trace (i) is the QNL, and traces (ii), (iii), and (iv) are the measured noise power spectra of the amplitude sum (phase difference) at 2 MHz for EPR1, EPR2, and EPR3, respectively. The initial correlation variances of EPR1 produced by NOPA1 are $\langle\delta^2(\hat{X}^{\rm out}_{a_1}+\hat{X}^{\rm out}_{a_2})\rangle = \langle\delta^2(\hat{Y}^{\rm out}_{a_1}-\hat{Y}^{\rm out}_{a_2})\rangle = 0.59$, corresponding to -5.3 ± 0.2 dB below the QNL. After the first-stage enhancement by NOPA2

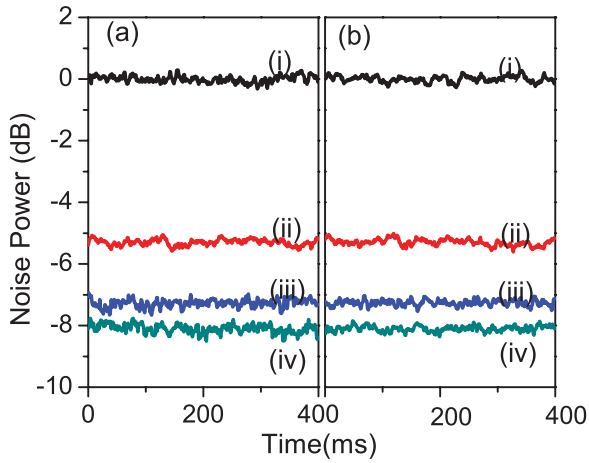

FIG. 4. (Color online) Noise powers of the correlation variances: (a) Trace (i), the QNL; trace (ii), correlation variance of $\langle\delta^2(\hat{X}^{\rm out}_{a_1}+\hat{X}^{\rm out}_{a_2})\rangle$; trace (iii), correlation variance of $\langle\delta^2(\hat{X}^{\rm out}_{b_1}+\hat{X}^{\rm out}_{b_2})\rangle$; trace (iv), correlation variance of $\langle\delta^2(\hat{X}^{\rm out}_{c_1}+\hat{X}^{\rm out}_{c_2})\rangle$. (b) Trace (i), the QNL; trace (ii), correlation variance of $\langle\delta^2(\hat{Y}^{\rm out}_{a_1}-\hat{Y}^{\rm out}_{a_2})\rangle$; trace (iii), correlation variance of $\langle\delta^2(\hat{Y}^{\rm out}_{b_1}-\hat{Y}^{\rm out}_{b_2})\rangle$; trace (iv), correlation variance of $\langle\delta^2(\hat{Y}^{\rm out}_{c_1}-\hat{Y}^{\rm out}_{c_2})\rangle$.

the correlation variances are reduced to $\langle\delta^2(\hat{X}^{\rm out}_{b_1}+\hat{X}^{\rm out}_{b_2})\rangle = \langle\delta^2(\hat{Y}^{\rm out}_{b_1}-\hat{Y}^{\rm out}_{b_2})\rangle = 0.38$, corresponding to -7.2 ± 0.2 dB below the QNL. At last, after the cascaded enhancement by NOPA2 and NOPA3, the correlation variances of EPR3 become $\langle\delta^2(\hat{X}^{\rm out}_{c_1}+\hat{X}^{\rm out}_{c_2})\rangle = \langle\delta^2(\hat{Y}^{\rm out}_{c_1}-\hat{Y}^{\rm out}_{c_2})\rangle = 0.31$, corresponding to -8.1 ± 0.2 dB below the QNL. The correlation variance of EPR3 is denoted in Fig. 2(a) with a red star, where $\gamma_1 = 0.1$, $\gamma_2 = 0.004$, $r = 0.83$ (-7.2 dB below the QNL) corresponding to the operation conditions of NOPA3. On trace (i) of Fig. 2(b) we can see that, when the correlation variance of the input EPR beam (EPR2) equals -7.2 dB, the correlation variance of the output field (EPR3) is -8.3 dB, which is in good agreement with the experimental measured value (-8.1 dB). We also measured the anticorrelation variances of EPR1, EPR2, and EPR3, which are $\langle\delta^2(\hat{X}^{\rm out}_{a_1}-\hat{X}^{\rm out}_{a_2})\rangle = \langle\delta^2(\hat{Y}^{\rm out}_{a_1}+\hat{Y}^{\rm out}_{a_2})\rangle = 13.6$, $\langle\delta^2(\hat{X}^{\rm out}_{b_1}-\hat{X}^{\rm out}_{b_2})\rangle = \langle\delta^2(\hat{Y}^{\rm out}_{b_1}+\hat{Y}^{\rm out}_{b_2})\rangle = 25.9$, and $\langle\delta^2(\hat{X}^{\rm out}_{c_1}-\hat{X}^{\rm out}_{c_2})\rangle = \langle\delta^2(\hat{Y}^{\rm out}_{c_1}+\hat{Y}^{\rm out}_{c_2})\rangle = 34.2$ corresponding to 8.3, 11.1, and 12.3 dB above the QNL, respectively. The sums of the amplitude and the phase correlation variances for EPR1, EPR2 and EPR3 are 1.18, 0.76, and 0.62, respectively, all of which satisfy the inseparability criterion, i.e., these values are smaller than 4 (when the sum is larger than 4 the signal and the idler optical modes in the output field are separable and thus do not form an entangled state) [8,9].

In conclusion, we have experimentally demonstrated that the CV entanglement of optical field can be enhanced by the cascaded NOPA. The upper limitation of the enhanced entanglement depends on the intracavity loss (γ_2) of the NOPA and the relative phase fluctuation θ of the phase-locking system. The presented scheme opens an avenue to enhance CV entanglement by using easily reachable optical devices. Besides, the presented cascaded system perhaps can

be used as a part of a particular quantum information protocol, where the entanglement needs to be successively enhanced step by step, which could be an open question for further study.

This research was supported by the National Basic Research Program of China (Grant No. 2010CB923103), the Natural Science Foundation of China (Grants No. 60736040, No. 11074157, and No. 61121064), and the TYAL.

[1] A. Galindo and M. A. Martin-Delgado, Rev. Mod. Phys. **74**, 347 (2002).
[2] S. L. Braunstein and P. van Loock, Rev. Mod. Phys. **77**, 513 (2005).
[3] M. D. Reid *et al*., Rev. Mod. Phys. **81**, 1727 (2009).
[4] D. Bouwmeester *et al*., Nature (London) **390**, 575 (1997).
[5] A. Furusawa *et al*., Science **282**, 706 (1998).
[6] A. Einstein, B. Podolsky, and N. Rosen, Phys. Rev. **47**, 777 (1935).
[7] M. D. Reid, Phys. Rev. A **40**, 913 (1989).
[8] L. M. Duan, G. Giedke, J. I. Cirac, and P. Zoller, Phys. Rev. Lett. **84**, 2722 (2000).
[9] R. Simon, Phys. Rev. Lett. **84**, 2726 (2000).
[10] L. A. Wu, H. J. Kimble, J. L. Hall, and H. Wu, Phys. Rev. Lett. **57**, 2520 (1986).
[11] A. M. Lance, T. Symul, W. P. Bowen, B. C. Sanders, and P. K. Lam, Phys. Rev. Lett. **92**, 177903 (2004).
[12] Y. Takeno, M. Yukawa, H. Yonezawa, and A. Furusawa, Opt. Express **15**, 4321 (2007).
[13] T. Eberle *et al*., Phys. Rev. Lett. **104**, 251102 (2010).
[14] M. Mehmet, H. Vahlbruch, N. Lastzka, K. Danzmann, and R. Schnabel, Phys. Rev. A **81**, 013814 (2010).
[15] M. Mehmet *et al*., Opt. Express **19**, 25763 (2011).
[16] T. Eberle *et al*., Phys. Rev. A **83**, 052329 (2011).
[17] M. Yukawa, R. Ukai, P. van Loock, and A. Furusawa, Phys. Rev. A **78**, 012301 (2008).
[18] Z. Y. Ou, S. F. Pereira, H. J. Kimble, and K. C. Peng, Phys. Rev. Lett. **68**, 3663 (1992).
[19] X. Y. Li *et al*., Phys. Rev. Lett. **88**, 047904 (2002).
[20] X. J. Jia *et al*., Phys. Rev. Lett. **93**, 250503 (2004).
[21] J. Laurat, T. Coudreau, G. Keller, N. Treps, and C. Fabre, Phys. Rev. A **71**, 022313 (2005).
[22] A. S. Villar, L. S. Cruz, K. N. Cassemiro, M. Martinelli, and P. Nussenzveig, Phys. Rev. Lett. **95**, 243603 (2005).
[23] J. T. Jing, S. Feng, R. Bloomer, and O. Pfister, Phys. Rev. A **74**, 041804 (2006).
[24] G. Keller *et al*., Opt. Express **16**, 9351 (2008).
[25] Y. Wang *et al*., Opt. Express **18**, 6149 (2010).
[26] H. X. Chen and J. Zhang, Phys. Rev. A **79**, 063826 (2009).
[27] Y. N. Shang, X. J. Jia, Y. M. Shen, C. D. Xie, and K. C. Peng, Opt. Lett. **35**, 853 (2010).
[28] J. Zhang, C. D. Xie, and K. C. Peng, Phys. Lett. A **299**, 427 (2002).
[29] T. C. Zhang, K. W. Goh, C. W. Chou, P. Lodahl, and H. J. Kimble, Phys. Rev. A **67**, 033802 (2003).